Superattracting extraneous fixed points and n-cycles for Chebyshev's method on cubic polynomials*

José M. Gutiérrez and Juan L. Varona

Departamento de Matemáticas y Computación, Universidad de La Rioja,
Complejo Científico-Tecnológico, Madre de Dios 53, 26006-Logroño, Spain
Emails: jmguti@unirioja.es, jvarona@unirioja.es

Abstract

In this work we provide analytic and graphic arguments to explain the behaviour of Chebyshev's method applied to cubic polynomials in the complex plane. In particular, we study the parameter plane related to this method and we compare it with other previously known, such as Newton's or Halley's methods. Our specific interest is to characterize "bad" polynomials for which Chebyshev's method presents convergence to points distinct from the roots (i.e. the root-finding algorithm fails). In particular, we prove the existence of polynomials for which Chebyshev's method has superattracting n-cycles and the existence of polynomials for which Chebyshev's method has superattracting extraneous fixed points. The first fact is shared with other root-finding methods, such as Newton's or Halley's, but the second one is an established dynamic feature of Chebyshev's method. Here we go depth on the study of the dynamics related to the superattracting n-cycles of Chebyshev's method and its relationships with the superattracting extraneous fixed points, providing some analytical and geometric arguments to explain the related parameter plane. In particular, we prove the existence of a sequence of parameters for which the corresponding Chebyshev's iterative method has a superattracting n-cycle.

Keywords: Chebyshev's method, parameter plane, dynamical systems, Mandelbrot-like sets.

MSC (2010): Primary 37F10; Secondary 65H05.

1 Introduction

The study of the dynamical behaviour of iterative methods for solving nonlinear equations in the complex plane is a subject that has drawn the attention of researchers in the last decades. Papers [1], [11], [16] or [18] and the references therein are a good evidence of this fact. The seminal works of Cayley and Schröder at the end of the 19th century, dealing with Newton's method applied to quadratic polynomials, were the beginning of a theory (iteration of rational functions) that has been in continuous evolution. The application of root-finding methods to polynomial equations leads to rational maps defined in the extended complex plane. Therefore, the theory and concepts related

*This paper has been published as: J. M. Gutiérrez and J. L. Varona, Superattracting extraneous fixed points and n-cycles for Chebyshev's method on cubic polynomials, *Qual. Theory Dyn. Syst.* **19** (2020), no. 2, article 54, 23 pp., https://doi.org/10.1007/s12346-020-00390-5

with the iteration of rational maps (see [3, 7, 12, 15]) can be applied in this situation. We assume that these concepts are known by the reader and we do not proceed to explain them in detail.

The dynamics of Newton's method for complex polynomials, mainly with low degree, have been profusely studied by different authors. One of the pioneer works in this field was the paper of Curry, Garnett and Sullivan [7], that eventually led to many other future studies (see [16], [19] or [21] as a sample). Other iterative methods, such as Halley's method, has also been considered (see [16] or [20], for instance). There is a plethora of iterative methods to be considered, each one with its own properties and particularities. Not in vain, Halley's and Chebyshev's methods are members of the well known families of Schröder iteration function of first and second kind respectively. The m-th member of each of these families is an iterative method with order of convergence m.

In this paper, we have chosen Chebyshev's method, a well-known third-order iterative method, whose dynamical properties show some surprises. Actually, even for polynomials of low degree, Chebyshev's method presents a dynamical behaviour that differs from the aforementioned Newton's or Halley's methods. Even for the simplest case of quadratic polynomials, Chebyshev's method does not satisfy the principle of nearest root principal, that holds for the other two methods (see [9], [10] or [19]); this property, proved by Cayley for quadratic polynomials with Newton's method, means that the orbit of an initial seed converges to the closest root, leaving the perpendicular bisector between the two roots as an invariant set where convergence fails. It is known [11] that in the case of Chebyshev's method applied to quadratics, the perpendicular bisector between the two roots is still invariant and the convergence to the roots fails in it. Therefore it is strictly contained in the Julia set. The Fatou set of Chebyshev's method applied to quadratics has got infinite components. This is another difference with Newton's or Halley's methods, where the Fatou set just has two components.

But even more, unlike other classical iterative methods, such us Newton's or Halley's, we can find polynomials with degree at least three for which Chebyshev's method presents convergence to situations different from the roots of the considered polynomial, such as attractive cycles of attractive extraneous fixed points. This fact was first established by Vrscay (see [19] or [20] for more details) and in this paper we are going to analyze in depth this subject; see, in particular, the behavior described in Theorem 4.

For a given nonlinear equation of the form $f(z) = 0$ and for a given $z_0 \in \mathbb{C}$, Chebyshev's method is defined recursively by $z_{n+1} = C_f(z_n)$, where

$$C_f(z) = z - \left(1 + \frac{1}{2} L_f(z)\right) \frac{f(z)}{f'(z)}, \tag{1}$$

with $L_f(z) = f(z)f''(z)/f'(z)^2$. Throughout this paper it will be convenient for us to introduce the operator L_f that maps a function f into the quotient

$$L_f : f \mapsto \frac{ff''}{(f')^2}. \tag{2}$$

Under appropriate conditions for the initial point z_0 and the involved functions f, the sequence $(z_n)_{n\geq 0}$ defined by the iteration of Chebyshev's map converges to a root of the equations $f(z) = 0$. The numerical properties of this rootfinding method (local and semilocal convergence, order of convergence, error estimates, computational efficiency and so on) have been profusely studied by different authors (see [2] or [8] for instance). In addition, these studies have been carried out for solving nonlinear equations not only defined in the complex plane, but also in the real line, in a n-dimensional setting or even in Banach spaces.

In order to make the paper as self-contained as posible, we remind some concepts about the iteration of a rational function R defined in the complex plane (see [3] for more details). It is said that $\zeta \in \mathbb{C}$ is a fixed point of R if $R(\zeta) = \zeta$. The fixed point ζ is classified as superattracting, attracting or repelling if $|R'(\zeta)|$ is 0, belongs to the interval $(0, 1)$ or is bigger than 1, respectively. If $|R'(\zeta)| = 1$, ζ is said indifferent.

It is said that $\zeta \in \mathbb{C}$ is a periodic point of R if it is a fixed point of some iterated function R^m, for $m \in \mathbb{N}$. Moreover, we say that ζ has period n if and only if it is a fixed point of R^n but not of R^k for any $k < n$. In this case, the set

$$\{\zeta, R(\zeta), R^2(\zeta), \ldots, R^{n-1}(\zeta)\}$$

is called an n-cycle of R. A periodic point ζ of R with period n can be classified as a fixed point of R^n with the same criterium explained above. If there exist attracting (superattracting) periodic cycles, then for initial data near the cycle the corresponding iteration of the rational function converge to this cycle and no to a root.

Let us assume that R is a rational function related to a root-finding method for solving a polynomial equation $f(z) = 0$. For instance, R could be the rational function C_f given in (1) for Chebyshev's method or for any other iterative method applied. We say that ζ is an extraneous fixed point of R if is a fixed point of R but is not a root of $f(z) = 0$. The same classification in superattracting, attracting, indifferent or repelling is also valid for extraneous fixed points.

It is well known ([11]) that the rational Newton map $z - f(z)/f'(z)$ has no extraneous fixed points and Halley's map $z - (2/(2 - L_f(z)))f(z)/f'(z)$ has only repelling extraneous fixed points. The existence of extraneous fixed points for Chebyshev's method (1) was also pointed out by Kneisl ([11]), but it is said that its characterization is most often not satisfied. However, in this paper we have been able to specify the cubical polynomials for which Chebyshev's method has superattracting extraneous fixed points.

A point ζ is said a critical point of a rational map R if R fails to be injective in any neighbourhood of ζ. It is well known that if R is a rational map with degree d, it has $2d-2$ critical points counted with multiplicities.

In this paper we follow the steps given by Roberts and Horgan-Kobelski ([16] for more details) in the dynamical study of Newton's and Halley's methods. In fact, we provide analytic and graphic arguments to explain the behaviour of Chebyshev's method applied to cubic polynomials. Let us denote $C_{p_\lambda}(z)$ to the rational map obtained by applying Chebyshev's method (1) to cubic polynomials in the form

$$p_\lambda(z) = (z^2 - 1)(z - \lambda), \quad \lambda \in \mathbb{C}. \tag{3}$$

There are other one-parameter families of cubic polynomials that could be used for studying the dynamics of iterative methods applied to cubic polynomilas, such as $(z^2 - z)(z - \rho)$, $\rho \in \mathbb{C}$, or $z^3 - (1 - \mu)z + \mu$, $\mu \in \mathbb{C}$. The advantage of the family (3) is its symmetry about the imaginary axis. This fact is very important to simplify our study.

We are interested in analyzing the space known as parameter space, obtained by following the orbits of the two free critical points of $C_{p_\lambda}(z)$. The critical points of $C_{p_\lambda}(z)$ which do not correspond to roots of $p_\lambda(z)$ are called free critical points of $C_{p_\lambda}(z)$. We color the λ-plane depending on the convergence of these two free critical points to any of the three roots of the polynomial p_λ, leading to $3^2 = 9$ possible color schemes. The strategy of following the orbits of the critical points is based in the following classical theorem (see [3]):

Theorem 1 (Fatou-Julia)**.** *Every attracting cycle of a rational map attracts at least one critical point.*

Our main goal is to find "bad" polynomials for Chebyshev's method, that is, polynomials for which this iterative method presents convergence to points different of the roots. We show the existence of parameters λ such that polynomial (3) is a bad polynomial for Chebyshev's method. To be more precise, we characterize polynomials (3) that give rise to superattracting n-cycles, for each $n \in \mathbb{N}$, $n \geq 2$, or to superattracting extraneous fixed points. The first fact is shared with other root-finding methods, such as Newton's or Halley's, as it was proved in [16] or [20]. However, as it was first pointed out by Vrscay [19] and next by García-Olivo et al [9], the existence of extraneous fixed points is a dynamical behaviour that appears in Chebyshev's method but not in Newton's or Halley's method.

Before undertaking our study, we mention some important features related with Chebyshev's method. All of them are straightforward calculations.

1. **(Scaling theorem).** Let $A(z) = \alpha z + \beta$ with $\alpha \neq 0$ be an affine map and let p and q two polynomials related by $q(z) = p(A(z))$. Then Chebyshev's iteration map C_p is conformal conjugate to C_q, namely $A \circ C_q \circ A^{-1} = C_p$.

2. Let $\nu(z) = \bar{z}$ be the usual complex conjugation. Suppose that $p(z) = \prod_j (z - r_j)$ and let us define $q(z) = \prod_j (z - \bar{r_j})$. Then C_p is topologically conjugate to C_q, namely $\nu \circ C_p = C_q \circ \nu$.

3. Chebyshev's method applied to polynomials of degree d gives rise to a rational function C_p, with $\deg(C_p) \leq 3d - 2$. Note that a combination of the summands of C_p yields

$$C_p(z) = \frac{2zp'(z)^3 - 2p(z)p'(z)^2 - p(z)^2 p''(z)}{2p'(z)^3}.$$

   For $d \geq 2$, if $p(z)$ and $p'(z)$ have simple roots, the rational function C_p has degree $3d-2$ because the numerator is a sum of terms of degree $3d-2$ whereas the denominator has degree $3d-3$. In addition, the leading coefficient of the numerator does not vanish. Indeed if we assume without loss of generality that $p(z)$ is monic, the leading coefficient is $d(d-1)(2d-1) \neq 0$. The rational map C_p has degree less than $3d-2$ if $p(z)$ or $p'(z)$ have multiple roots.

4. Simple roots of p are superattracting fixed points of C_p. Even more, if z^* is a simple root of p, then $C_p'(z^*) = C_p''(z^*) = 0$, so the iterative root-finding algorithm is cubically convergent.

5. The derivative of Chebyshev's iteration map (1) is

$$C_p'(z) = \frac{(3 - L_{p'}(z))L_p(z)^2}{2}, \tag{4}$$

   where $L_{p'}(z) = p'(z)p'''(z)/p''(z)^2$, according the notation introduced in (2).

6. Chebyshev's method has linear convergence for roots z^* with multiplicity $m > 1$. In this case

$$C_p'(z^*) = \frac{(m-1)(2m-1)}{2m^2} \in (0, 1).$$

7. Chebyshev's method could have extraneous fixed points, i.e., fixed points of C_p that are not roots of p; of course the appearance of these points may complicate the root-finding method, because they may trap an iteration sequence giving false roots. The extraneous fixed points are solutions of

$$L_p(z) = -2.$$

In addition, they are attracting if

$$|6 - 2L_{p'}(z)| < 1$$

and superattracting if $L_{p'}(z) = 3$. Note that these characterizations coincide with the ones given by Kneisl [11, Theorem 2.6.4] and also by Vrscay [20, page 12], although for a different parametrization of cubic polynomials and with different techniques and notation (we make use of the functions L_p and $L_{p'}$).

8. The point at infinity is a repelling fixed point for Chebyshev's method applied to polynomials of degree d. Observe that in all the cases considered in the above third item, the degree of the numerator of C_p is bigger than the degree of the denominator of C_p (just in a unit). So the point at infinity is a fixed point of C_p, according the characterization given in [3, Sec. 2.6]. Even more, its multiplier is

$$\frac{1}{C_p'(\infty)} = \frac{2d^2}{(d-1)(2d-1)} > 1.$$

Note that $L_p(\infty) = (d-1)/d$ and $L_{p'}(\infty) = (d-2)/(d-1)$, so by (4) we have

$$\frac{1}{C_p'(\infty)} = \frac{2d^2}{(d-1)^2(3-(d-2)/(d-1))} = \frac{2d^2}{(d-1)(2d-1)}.$$

In particular, for cubic polynomials, ∞ is a repelling fixed point with multiplier $9/5$.

9. Taking into account (4), the solutions of $L_{p'}(z) = 3$ are critical points of C_p. Consequently, the solutions of $L_{p'}(z) = 3$ that are not roots of p are free critical points of C_p. It is important to observe that the inflection points of p are not free critical points of C_p, in contrast with Newton's method. Actually, if z^* satisfies $p''(z^*) = 0$, then the pole of order 2 of $L_{p'}(z)$ in (4) cancels the double root from $L_p(z)^2$. Consequently, in this case

$$C_p'(z^*) = -\frac{p(z^*)^2 p'''(z^*)}{2p'(z^*)^3}.$$

2 Chebyshev's method applied to cubic polynomials

The dynamical study of Chebyshev's method applied to quadratic polynomials with different roots have been carried out in other previous works, as [5], [6] or [11]. Even in this first case, it is established that the Julia set for the Chebyshev's map is not the locus of points equidistant from the roots, as it happens in Newton's or Halley's method. So, from the very beginning, we note that the dynamics of Chebyshev's method deserves a particular study.

In [9] we find a first glance on the dynamics of Chebyshev's method in the cubic case. In [11] it is proved that Chebyshev's method is not generally convergent for cubics. General convergence of an iterative method is a concept introduced by Smale [17] and later generalized by McMullen [13]. It means that for almost every initial point and for almost every polynomial of a given degree, the method converges to a root of the considered polynomial. For instance, the map obtained by applying method (1) to the polynomial $p(z) = z^3 + z^2/2 + z/2 - 1/2$ has a superatracting fixed point at the origin, that is not any root of p.

In the current paper we present a new perspective of the behaviour of Chebyshev's method applied to cubic polynomials with at least two different roots, following the steps given by Roberts and Horgan-Kobelski for Newton's or Halley's methods [16]. As a first step, we highlight that the use of the Scaling theorem reduces (see [1]) the problem to the study of Chebyshev's method applied to the one-parameter family of polynomials (3). That is, for any cubic polynomial $q(z)$ with at least two distinct roots, there exists a parameter $\lambda \in \mathbb{C}$ such that Chebyshev's map for q, C_q, is conformal conjugate to C_{p_λ}, with p_λ defined in (3).

Chebyshev's map for polynomials p_λ is a rational function of degree less than or equal to seven

$$C_{p_\lambda}(z) = \frac{H_\lambda(z)}{(3z^2 - 2\lambda z - 1)^3},$$

where $H_\lambda(z) = 15z^7 - 26\lambda z^6 + 15\lambda^2 z^5 - 6z^5 - 3\lambda^3 z^4 - 9\lambda z^4 + 18\lambda^2 z^3 - z^3 - 6\lambda^3 z^2 + 12\lambda z^2 - 9\lambda^2 z + \lambda^3 - \lambda$. Note that if $\lambda \neq \sqrt{3}i$, C_{p_λ} has two free critical points. Actually, by (4) these free critical points satisfy $L_{p'}(z) = 3$, that is $p'(z)p'''(z) = 3p''(z)^2$ or, equivalently,

$$15z^2 - 10\lambda z + 1 + 2\lambda^2 = 0.$$

This equation has two solutions:

$$\rho_-(\lambda) = \frac{5\lambda - \sqrt{-5(\lambda^2+3)}}{15}, \quad \rho_+(\lambda) = \frac{5\lambda + \sqrt{-5(\lambda^2+3)}}{15}. \tag{5}$$

In the above formulas, the squared root is defined with the principal argument.

If $\lambda = \sqrt{3}i$, Chebyshev's iteration map applied to the polynomial $(z^2-1)(z-\sqrt{3}i)$ yields the rational map

$$C_{p_{\sqrt{3}i}}(z) = \frac{15z^7 - 26i\sqrt{3}z^6 - 51z^5 - 55z^3 + 30i\sqrt{3}z^2 + 27z - 4i\sqrt{3}}{\left(\sqrt{3}z - i\right)^6}.$$

In this case,

$$C'_{p_{\sqrt{3}i}}(z) = \frac{15\left(z - i\sqrt{3}\right)^2\left(z^2-1\right)^2}{\left(\sqrt{3}z - i\right)^6},$$

then Chebyshev's iteration map has no free critical points and the only attracting behaviours are due to the three roots of the polynomial.

The strategy is to color the complex plane (that in this context is known as *parameter plane*) depending on the behaviour of the orbits of the two free critical points defined in (5) under the iteration of C_{p_λ}; that is, the color of the point λ in the complex plane depends on the behavior of the orbit of $\rho_\pm(\lambda)$ for C_{p_λ}. As there are two free critical points and three roots, we can find $3^2 = 9$ possible convergence schemes, as shown in Table 1. For instance, λ is colored in blue when the orbit of the critical point $\rho_-(\lambda)$ converges to the root -1 and the orbit of the critical point $\rho_+(\lambda)$ converges to the root 1. Figure 1 shows a part of the parameter plane of Chebyshev's method applied to cubic polynomials (3). On the left figure, we can appreciate the symmetry about the real axis, a question that could be deduced from the properties of the complex conjugation.

As in the case of other iterative methods, such as Newton's or Halley's methods, we can find black zones in the parameter plane corresponding to points λ for which one of the two free critical points does not converge to a root. These black zones are small Mandelbrot sets, as it is usual in

Color	$(\rho_-(\lambda), \rho_+(\lambda)) \to$	Color	$(\rho_-(\lambda), \rho_+(\lambda)) \to$
Yellow	$(-1, -1)$	Blue	$(-1, 1)$
Green	$(1, -1)$	Red	(λ, λ)
Brown	$(-1, \lambda)$	Pink	$(\lambda, -1)$
Orange	$(1, 1)$	Cyan	$(\lambda, 1)$
Purple	$(1, \lambda)$		

Table 1: Coloring scheme for Chebyshev's method applied to polynomials $(z^2 - 1)(z - \lambda)$, $\lambda \in \mathbb{C}$, according to the convergence of the two free critical points $\rho_-(\lambda)$ and $\rho_+(\lambda)$ defined in (5). For example, λ is colored in blue if the orbit of $\rho_-(\lambda)$ converges to the root -1 and the orbit of $\rho_+(\lambda)$ converges to the root 1.

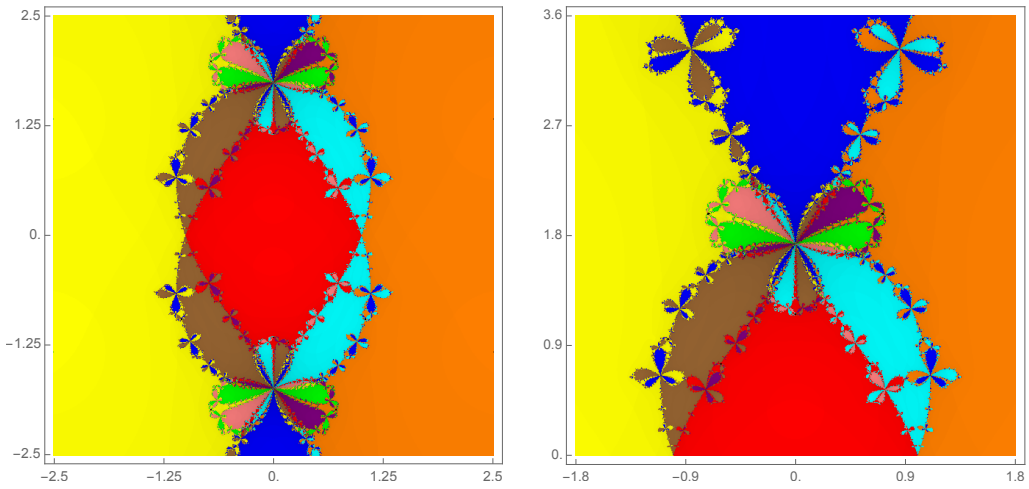

Figure 1: On the left, a square $[-2.5, 2.5] \times [-2.5, 2.5]$ of the parameter plane for Chebyshev's method applied to cubic polynomials, colored according to the color scheme indicated in Table 1; it shows the symmetry about the real axis. On the right, a square $[-1.8, 1.8] \times [0.0, 3.6]$ of the same parameter plane.

the iteration of one-parameter families of rational maps where a bifurcation occurs (see [14] and the recent paper [4] for more information about the universality of the Mandelbrot set). In the case of Newton's or Halley's methods, these black zones are due to the existence of attracting n-cycles. But in the case of Chebyshev's method these black zones come from:

- The presence of attracting extraneous fixed points. Note that it is not possible to find attracting extraneous fixed points in Newton's or Halley's methods. (As long as we know, the existence of extraneous fixed points produced by root-finding methods has been found, by the fist time, by Vrscay in [19], in the context of Schröder rational iteration functions.)

- The presence of attracting n-cycles. The presence of attracting n-cycles is a dynamical property that also happens in Newton's and Halley's methods.

We prove these two points in the following sections. It is complicated to find these black holes in the parameter plane just by visual inspection (they are "small" regions). However after a few calculations, we can find some of them, as we prove in the foregoing sections.

For each value of λ in a black hole of the parameter plane, the corresponding Chebyshev's iterative function $C_{p_\lambda}(z)$ fails from a root-finding point of view. To be more specific, there exists open regions of initial seeds $z_0 \in \mathbb{C}$ for which the iterative method $z_{n+1} = C_{p_\lambda}(z_n)$ does not converge to any of the roots, as it can be seen in the dynamical planes shown in Section 3 (see Figures 9 and 10, for instance).

2.1 Superattracting extraneous fixed points for Chebyshev's method

According to the main properties of Chebyshev's method we have listed above, superattracting extraneous fixed points for Chebyshev's method are solutions of the system of nonlinear equations

$$\begin{cases} L_p(z) = -2, \\ L_{p'}(z) = 3 \end{cases}$$

that satisfy $p''(z) \neq 0$. For polynomials defined in (3) this system reduces to

$$\begin{cases} 12z^4 - 16z^3\lambda + 5z^2\lambda^2 - 9z^2 + 8z\lambda - \lambda^2 + 1 = 0, \\ 15z^2 - 10z\lambda + 2\lambda^2 + 1 = 0 \end{cases} \tag{6}$$

with $\lambda \neq 3z$ (precisely this inequality comes from the case $p''(z) \neq 0$). Although this system of equations can be deduced from the conditions given by Kneisl [11] or Vrscay and Gilbert [20], we go one step further, by solving it and by obtaining six different solutions (λ, z). By using Gröbner bases, the following equivalent system of equations can be deduced:

$$\begin{cases} 11532 + 16501\lambda^2 + 7813\lambda^4 + 1639\lambda^6 + 147\lambda^8 = 0, \\ 74400z - 65396\lambda - 30179\lambda^3 - 7754\lambda^5 - 735\lambda^7 = 0. \end{cases}$$

The first equation can be factorized as $(3 + \lambda^2)(4 + 3\lambda^2)(31 - 10\lambda + 7\lambda^2)(31 + 10\lambda + 7\lambda^2) = 0$, so their roots can be immediately computed. From the second equation we obtain z as a function of λ:

$$z = \frac{\lambda\left(735\lambda^6 + 7754\lambda^4 + 30179\lambda^2 + 65396\right)}{74400}.$$

Without considering the pairs $(\sqrt{3}i, \sqrt{3}i/3)$ and $(-\sqrt{3}i, -\sqrt{3}i/3)$, because $\lambda = 3z$ in these cases, we obtain the solutions (λ, z) given by

$$\lambda = \pm\frac{2\sqrt{3}}{3}\,i \approx \pm 1.154701i, \qquad z = \pm\frac{\sqrt{3}}{3}\,i \approx \pm 0.57735i \tag{7}$$

and

$$\lambda = \frac{\pm 5 \pm 8\sqrt{3}i}{7} \approx \pm 0.714286 \pm 1.979487i, \qquad z = \frac{\pm 3 \pm 2\sqrt{3}i}{7} \approx \pm 0.428571 \pm 0.494872i.$$

As far as we know, this characterization of superattracting extraneous fixed points for Chebyshev's method has not been previously done. Note that for each of these values of λ, the Chebyshev's map obtained for the polynomial $p_\lambda(z)$ defined in (3) has a superattracting extraneous fixed point

at the related value of z. This fact gives rise to the emergence of black holes in the parameter plane. Figure 2 shows two details of the the parameter plane of Chebyshev's method for cubic polynomials. In fact, we see the existence of Mandelbrot-like sets near two of these values of λ. In addition, in Figure 9 we have plotted the dynamical plane (basins of attraction) of Chebyshev's method applied to the polynomial given in (3), with $\lambda = (5 + 8\sqrt{3}i)/7$. We can distinguish the basins of attraction of the three roots together with the basin of the superattracting extraneous fixed point, colored in white (see Section 3 for more details).

Finally, it is worth noting that the set of λ-values obtained previously as solutions of the system (6) are related by some affine conjugacies. Actually, the map

$$T(z) = \frac{-2z + \lambda - 1}{1 + \lambda}$$

is an affine map of the complex plane satisfying $T(-1) = 1$, $T(\lambda) = -1$ and $T(1) = (\lambda - 3)/(\lambda + 1)$. Consequently $T(z)$ is an affine conjugacy between Chebyshev's method applied to p_λ and Chebyshev's method applied to p_{λ^*}, where

$$\lambda^* = \frac{\lambda - 3}{1 + \lambda}. \tag{8}$$

Plugging in $\lambda = \pm 2\sqrt{3}i/3$ into equation (8) gives $\lambda^* = (-5 \pm 8\sqrt{3}i)/7$, which are also solutions of the system (6).

A similar argument works by using the conjugacy map

$$S(z) = \frac{-2z + \lambda + 1}{1 - \lambda}$$

that satisfies $S(1) = -1$, $S(\lambda) = 1$ and $S(-1) = (\lambda + 3)/(1 - \lambda)$. In this case $S(z)$ is an affine conjugacy between Chebyshev's method applied to p_λ and Chebyshev's method applied to $p_{\lambda^{**}}$, where

$$\lambda^{**} = \frac{\lambda + 3}{1 - \lambda}. \tag{9}$$

If we writte $\lambda = \pm 2\sqrt{3}i/3$ into equation (9), we obtain $\lambda^{**} = (5 \pm 8\sqrt{3}i)/7$, the rest of solutions of the system (6).

2.2 Superattracting n-cycles for Chebyshev's method

Now, let us analyze the existence of superattracting n-cycles for Chebyshev's method C_{p_λ}, that is sets of n complex numbers $\{z_0, z_1, \ldots, z_{n-1}\}$ such that $z_k = C_{p_\lambda}(z_{k-1})$ for $1 \leq k \leq n-1$ and $z_0 = C_{p_\lambda}(z_k)$, with $(C^n_{p_\lambda})'(z_0) = 0$ where $C^n_{p_\lambda}$ is the composition of C_{p_λ} with itself n times. The length of the cycle is the least value of n that satisfies this property.

To do this, we restrict our study to the positive part of the imaginary axis, i.e. to Chebyshev's method applied to

$$p_\lambda(z) = (z^2 - 1)(z - \lambda), \quad \lambda = \beta i, \quad \beta \in \mathbb{R}^+.$$

Note that Chebyshev's method leaves the imaginary axis invariant, so it is enough to study the imaginary part of $C_{p_{\beta i}}(iy)$, $y \in \mathbb{R}$, that is,

$$R_\beta(y) = \frac{q(\beta, y)}{(3y^2 - 2\beta y + 1)^3}, \tag{10}$$

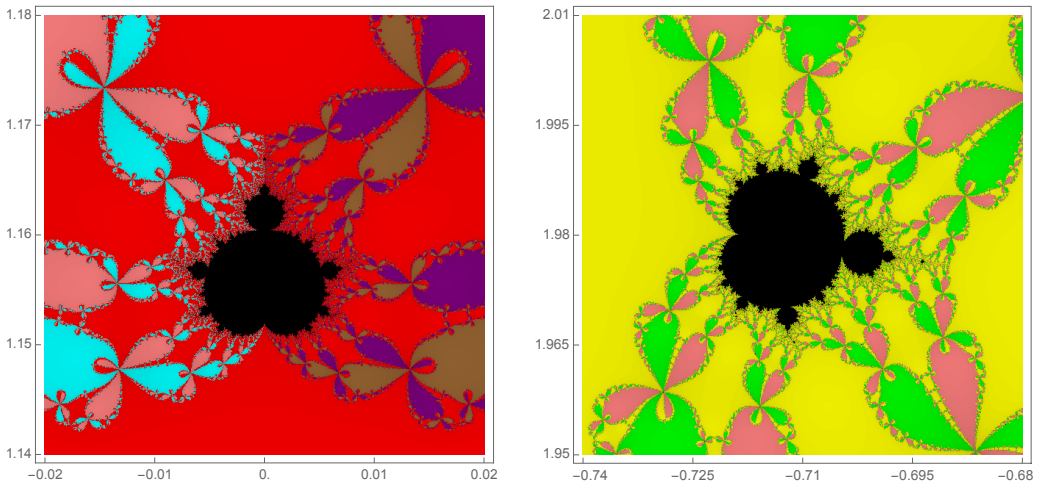

Figure 2: On the left, a rectangle $[-0.02, 0.02] \times [1.14, 1.18]$ containing a black hole coming from the superattracting extraneous fixed point related to the value $\lambda = \frac{2\sqrt{3}}{3}i$ in the parameter plane. On the right, a rectangle $[-0.74, -0.68] \times [1.95, 2.01]$ of the parameter plane containing a black hole coming from the superattracting extraneous fixed point related to $\lambda = \frac{-5+8\sqrt{3}i}{7}$.

where $q(\beta, y)$ is a seventh-degree polynomial in y with coefficients that depend on β:

$$q(\beta, y) = 15y^7 - 26y^6\beta + 15y^5\beta^2 + 6y^5 - 3y^4\beta^3 + 9y^4\beta - 18y^3\beta^2 - y^3 + 6y^2\beta^3 + 12y^2\beta - 9y\beta^2 + \beta^3 + \beta.$$

We simplify our study to the case $\beta \geq 0$. A similar study could be done for $\beta < 0$. The map R_β defined in (10) has the following properties:

- $R_\beta(\beta) = \beta$ for all $\beta \geq 0$.
- If $\beta > \sqrt{3}$, R_β has two poles: $\frac{1}{3}\left(\beta \pm \sqrt{\beta^2 - 3}\right)$.
- If $\beta \neq \sqrt{3}$, the derivative of the real valued function R_β is

$$R'_\beta(y) = \frac{3\left(y^2+1\right)^2(\beta - y)^2\left(15y^2 - 10\beta y + 2\beta^2 - 1\right)}{\left(3y^2 - 2\beta y + 1\right)^4}. \tag{11}$$

  Consequently, if $0 \leq \beta < \sqrt{3}$, R_β has two free critical points, the solutions of $15y^2 - 10\beta y + 2\beta^2 - 1 = 0$. Let us denote them by

$$\varrho_-(\beta) = \frac{1}{15}\left(5\beta - \sqrt{5(3-\beta^2)}\right), \quad \varrho_+(\beta) = \frac{1}{15}\left(5\beta + \sqrt{5(3-\beta^2)}\right). \tag{12}$$

  In fact, $\varrho_-(\beta)$ and $\varrho_+(\beta)$ are relative maximum and minimum of R_β respectively.

- If $\beta = \sqrt{3}$, R_β can be written in the form

$$R_{\sqrt{3}}(y) = \frac{5\sqrt{3}y^6 - 21y^5 + 10\sqrt{3}y^4 + 10y^3 - 15\sqrt{3}y^2 + 15y - 4\sqrt{3}}{\left(\sqrt{3}y - 1\right)^5}.$$

Consequently, there is just one pole at $\sqrt{3}/3$. In addition,

$$R'_{\sqrt{3}}(y) = \frac{15\left(y-\sqrt{3}\right)^2\left(y^2+1\right)^2}{\left(\sqrt{3}y-1\right)^6}$$

and there are not free critical points in this case.

- R_β has an oblique asymptote: $5y/9 + 4\beta/27$.
- Note that, from (7), if $\beta = 2\sqrt{3}/3 \approx 1.1547$ the equation $R_\beta(y) = y$ has solutions different from $y = \beta$ (extraneous fixed points). Equivalently, we can say that for this value of β the image by R_β of the relative minimum $\varrho_+(\beta)$ is under the diagonal. Actually, there is a value $\bar{\lambda} \approx 1.15209851$ for which the function R_β has extraneous fixed point for $\beta \geq \bar{\lambda}$. The value $\bar{\lambda}$ has been numerically obtained.

As a consequence, R_β has free critical points when it has no vertical asymptotes. To simplify our study, we reduce the domain of the parameter β to the case $[0, \sqrt{3})$, where the presence of free critical points is guaranteed. We follow the orbits of these free critical points with the aim of finding cycles. We summarize the main properties of the function R_β for $\beta \in [0, \sqrt{3})$ in the following lemma. A typical graph of R_β for $\beta \in [\bar{\lambda}, \sqrt{3})$ is shown on the left graphic of Figure 3.

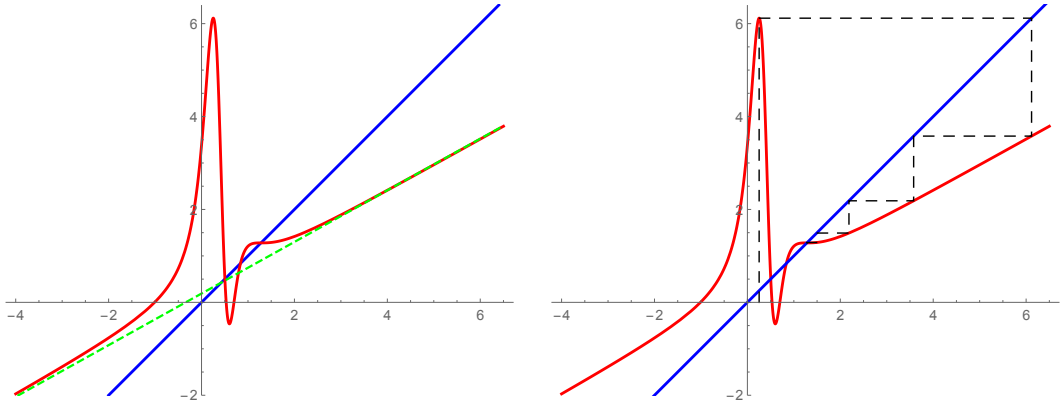

Figure 3: On the left, graph or $R_\beta(y)$ for $\beta = 1.28$ (note that y is the horizontal axis). It represents a typical graph of R_β for $\bar{\lambda} \leq \beta < \sqrt{3}$. We have also plotted the diagonal and the oblique asymptote (dashed). In this case, we note the presence of two repelling fixed points (at $y \approx 0.5027$ and $y \approx 0.8391$) together with the attracting fixed point at $y = \beta$. On the right, the web diagram showing the convergence of the free critical point $\varrho_-(\beta)$ to the fixed point β.

Lemma 2. *Let β be a parameter in the interval $[0, \sqrt{3})$ and R_β the function defined in (10). Then $R_\beta(y)$ is continuous for all $y \in \mathbb{R}$, it is increasing for $y \in (-\infty, \varrho_-(\beta)) \cup (\varrho_+(\beta), \infty)$ and it is decreasing for $y \in (\varrho_-(\beta), \varrho_+(\beta))$, where $\varrho_-(\beta)$ and $\varrho_+(\beta)$ are defined in (12). In addition, the image by R_β of the relative maximum $\varrho_-(\beta)$ tends to ∞ when $\beta \to \sqrt{3}$, whereas the image of the relative minimum $\varrho_+(\beta)$ tends to $-\infty$ when $\beta \to \sqrt{3}$.*

Proof. The continuity of $R_\beta(y)$ and its increasing/decreasing properties follow immediately from the definition (10) and the expression of the derivative (11). In addition, as

$$R_\beta(\varrho_-(\beta)) = \beta + \frac{\beta(661\beta^2+117)}{729(3-\beta^2)} + \frac{\sqrt{5}}{1458}\frac{23\beta^6+468\beta^4+1971\beta^2+54}{(3-\beta^2)^{5/2}},$$

we deduce that $\lim_{\beta\to\sqrt{3}^-} R_\beta(\varrho_-(\beta)) = \infty$. Let us define

$$h(\beta) = R_\beta(\varrho_+(\beta)). \tag{13}$$

Then

$$h(\beta) = -\frac{1}{1458(3-\beta^2)}\left(8\beta(17\beta^2-576) + \frac{\sqrt{5}(23\beta^6+468\beta^4+1971\beta^2+54)}{(3-\beta^2)^{3/2}}\right).$$

Note that $h(\beta)$ is continuous in $[0,\sqrt{3})$ and $\lim_{\beta\to\sqrt{3}^-} h(\beta) = -\infty$. □

The situation shown in the right graphic of Figure 3 is not an isolated behaviour. Actually, we can prove that the orbits of the free critical point $\varrho_-(\beta)$ converge to the fixed point β, for a wide range of values of β.

Lemma 3. *For $1/\sqrt{7} \le \beta < \sqrt{3}$, the orbit of the free critical point $\varrho_-(\beta)$ under iteration by R_β defined in* (10) *converges to the fixed point β, that is,*

$$\lim_{n\to\infty} R_\beta^n(\varrho_-(\beta)) = \beta.$$

Proof. First note that $R_\beta(\varrho_-(\beta)) > \beta$ because of the inequality

$$R_\beta(\varrho_-(\beta)) - \beta = \frac{\beta(661\beta^2+117)}{729(3-\beta^2)} + \frac{\sqrt{5}}{1458}\frac{23\beta^6+468\beta^4+1971\beta^2+54}{(3-\beta^2)^{5/2}} > 0$$

for $0 \le \beta < \sqrt{3}$. Secondly, by (11), $R'_\beta(y) > 0$ for all $y > \beta$. Note that this inequality happens for $y > \varrho_+(\beta)$, but $\varrho_+(\beta) \le \beta$ because the inequality $1/\sqrt{7} \le \beta$ holds from the hypothesis.

Finally, we have $R_\beta(y) < y$ for all $y > \beta$. Actually,

$$R_\beta(y) - y = -\frac{\left(y^2+1\right)(y-\beta)\left(12y^4-16\beta y^3+5\beta^2y^2+9y^2-8\beta y+\beta^2+1\right)}{\left(3y^2-2\beta y+1\right)^3} < 0$$

because all the factors that appear in this quotient are positive for $y > \beta$. Note that the polynomial $u(y) = 12y^4-16\beta y^3+5\beta^2y^2+9y^2-8\beta y+\beta^2+1$ is strictly positive in the interval $[\beta,\infty)$. Indeed, $u(\beta) = (\beta^2+1)^2$ and

$$u'(y) = 48y^2(y-\beta) + 2(5\beta^2+9)y - 8\beta > 0 \quad \text{if} \quad y > \beta.$$

Let us iterate $y_{n+1} = R_\beta(y_n)$ starting with $y_0 = \varrho_-(\beta)$. Then $y_1 = R_\beta(\varrho_-(\beta)) > \beta$. It follows that R_β maps the interval $[\beta,\infty)$ into itself. In addition, as $R'_\beta(y) > 0$ and $R_\beta(y) < y$ for $y > \beta$, the sequence $\{y_n\}_{n\ge0}$ is strictly decreasing and bounded below by β. So it converges to a certain limit in $[\beta,\infty)$. As β is the only fixed point of the map R_β in $[\beta,\infty)$, the sequence $\{y_n\}_{n\ge0}$ converges to β. □

Remark 1. The behaviour of the orbit of the free critical point $\varrho_-(\beta)$ for $\beta \in [0, 1/\sqrt{7})$ is slightly different. In this case, $\beta < \varrho_+(\beta)$ and the interval $[\beta, \infty)$ is mapped into the interval $[R_\beta(\varrho_+(\beta)), \infty) \supset [\beta, \infty)$. There are not extraneous fixed points in this situation. The superattracting character of β, the only real fixed point of R_β, guarantees the convergence of the orbits $R_\beta^n(\varrho_-(\beta))$ to β, although perhaps in a non strictly decreasing way.

As a consequence of Lemma 3, the only option for finding superattracting n-cycles is to follow the orbits of the free critical point

$$\varrho_+(\beta) = \frac{1}{15}\left(5\beta + \sqrt{5(3-\beta^2)}\right).$$

Actually, for each $n \geq 2$, we define the function

$$g_n(\beta) = R_\beta^n(\varrho_+(\beta)) - \varrho_+(\beta). \tag{14}$$

A root of $g_n(\beta) = 0$ that is not a root of $g_k(\beta) = 0$ for $k < n$ gives rise to a superattracting n-cycle of R_β. Table 2 contains some approximate solutions, β_n, of the equation $g_n(\beta) = 0$ for different values of n. The following result establishes the existence of an increasing sequence of values for β_n. This sequence converges to $\sqrt{3} \approx 1.73205$. Consequently, for each of these values β_n, Chebyshev's method applied to polynomials in the form $(z^2-1)(z-\beta_n i)$ has superattracting n-cycles.

n	2	3	4	5	6	7	8	9	10
β_n	1.28657	1.34015	1.38943	1.43776	1.48369	1.52557	1.56245	1.59405	1.62056
n	11	12	13	14	15	16	17	18	19
β_n	1.64248	1.66038	1.67488	1.68656	1.69591	1.70338	1.70932	1.70932	1.71780
n	20	21	22	25	30	35	40	45	50
β_n	1.72078	1.72313	1.72500	1.72856	1.73097	1.73172	1.73195	1.73202	1.73204

Table 2: Some (approximate) solutions of the equation $g_n(\beta) = 0$, with g_n defined in (14).

Theorem 4. *For each integer $n \geq 2$, there exists a parameter value β_n, with $\beta_n > 1$, such that the orbit of the free critical point*

$$\varrho_+(\beta_n) = \frac{1}{15}\left(5\beta_n + \sqrt{5(3-\beta_n^2)}\right)$$

under iteration of R_β defined in (10) *forms a superattracting n-cycle. In addition, the sequence β_n is strictly increasing and $\lim_{n\to\infty} \beta_n = \sqrt{3}$.*

Proof. Let us consider the function $h(\beta)$ defined in (13). In addition to the properties shown in Lemma 2, we have that, for $0 \leq \beta < \sqrt{3}$,

$$h''(\beta) = -\frac{105\left(7\beta^2-1\right)^2\left(\beta^4+9\beta^2+64\right)^2}{2\left(3-\beta^2\right)^{9/2}\left(400\beta\left(\beta^2+9\right)\left(3-\beta^2\right)^{3/2}+\sqrt{5}\left(61\beta^6+2826\beta^4+8397\beta^2+1728\right)\right)} \leq 0,$$

so $h(\beta)$ is a concave function in the interval $[0, \sqrt{3})$ with the shape shown in the left graphic of Figure 4. Then, the equation $h(\beta) = 0$ has two solutions in the interval $[0, \sqrt{3})$. Let us denote

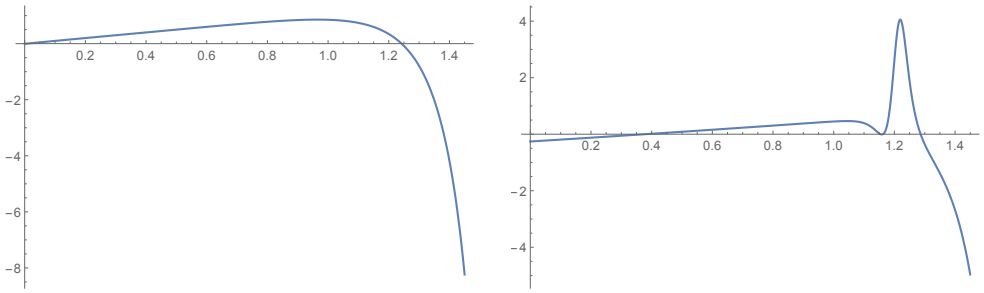

Figure 4: On the left, graph of the function $h(\beta)$ defined in (13). On the right, graph of the function $g_2(\beta)$ defined in (14). We see that there are four solutions of $g_2(\beta) = 0$.

$\beta^* \approx 1.2424$ the biggest one of these solutions (this value has been numerically obtained). So, if $\beta > \beta^*$, $h(\beta) < 0$ and $h(\beta)$ decreases monotonically to $-\infty$ when β increases towards $\sqrt{3}$.

Let us consider the function $g_2(\beta)$ defined in (14) and whose graphic appears in the right side of Figure 4. It has four zeros in the interval $[0, \sqrt{3})$: 0.37796, 1.15470, 1.16207 and 1.28657. Let us take β_2 as the biggest of these roots, i.e., $\beta_2 \approx 1.28657$. Note that $\beta_2 > \beta^*$ and then $h(\beta_2) < 0$.

It is possible to numerically approach some other values of β_n for $n \geq 3$. Some of them are shown in Table 2. But we can also give a proof of the existence of these values. Figure 5 (left) shows the graphs or R_β for $\beta = 1.28657$, and Figure 6 (left) for $\beta = 1.34015$. These graphics show a typical graph of a function R_β defined in (10), for $\beta \in (0, \sqrt{3})$, with no asymptotes, a maximum at $\varrho_-(\beta)$ and a minimum at $\varrho_+(\beta)$. When $\beta \to \sqrt{3}$, the two free critical points collapse in the value $\sqrt{3}/3$ that becomes an asymptote of the corresponding function R_β.

Let us analyze in detail the left graphic in Figure 5. The orbit of the free critical point $\varrho_+(\beta_2)$ gives rise to a superattracting 2-cycle. As the function $h(\beta)$ defined in (13) is decreasing in the interval $(\beta^*, \sqrt{3})$, if we consider a value $\beta > \beta_2 > \beta^*$, we have that the image of the corresponding critical point moves down, that is, $R_\beta(\varrho_+(\beta)) < R_{\beta_2}(\varrho_+(\beta_2))$. In addition, $R^2_\beta(\varrho_+(\beta)) < \varrho_+(\beta_2)$. So the value of $R^2_\beta(\varrho_+(\beta))$ has moved to the left, avoiding to close the 2-cycle. If we continue increasing β, the value of $R^2_\beta(\varrho_+(\beta))$ keeps moving to the left. This process can be seen in Figure 5. Taking into account the shape of the functions $R_\beta(y)$ shown in Lemma 2, we claim that there exists a value of $\hat{\beta}_2$ for which $R^2_{\hat{\beta}_2}(\varrho_+(\hat{\beta}_2))$ reaches the other free critical point, $\varrho_-(\hat{\beta}_2)$. For this value, we have

$$R^3_{\hat{\beta}_2}(\varrho_+(\hat{\beta}_2)) = R_{\hat{\beta}_2}(\varrho_-(\hat{\beta}_2)) > \hat{\beta}_2 > \varrho_+(\hat{\beta}_2).$$

Then $g_3(\hat{\beta}_2) > 0$. But $g_3(\beta)$ is a continuous function in $[0, \sqrt{3})$ that satisfies

$$\lim_{\beta \to \sqrt{3}^-} g_3(\beta) = -\infty,$$

consequently there exists at least one value β_3 such that $\beta_2 < \hat{\beta}_2 < \beta_3 < \sqrt{3}$ and $g_3(\beta_3) = 0$. If there exist several solutions of $g_3(\beta) = 0$, we choose β_3 as the biggest one.

We can reproduce this reasoning to inductively establish that if β_n is a solution of $g_n(\beta) = 0$, there exists a solution β_{n+1} of $g_{n+1}(\beta) = 0$, just by establishing the existence of $\hat{\beta}_n$ such that

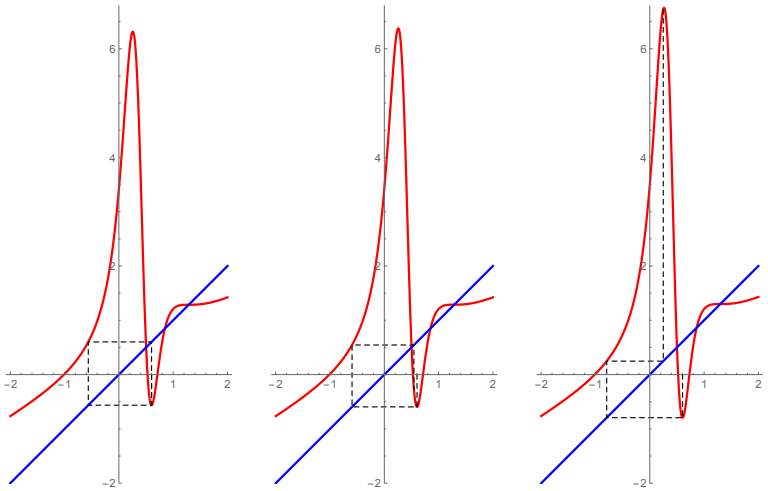

Figure 5: On the left, graph or $R_\beta(y)$ for $\beta = \beta_2 \approx 1.28657$ together with the web diagram proving the existence of a superattracting 2-cycle containing the free critical point $\varrho_+(\beta_2)$. In the middle, graph or $R_\beta(y)$ for $\beta = 1.2885$. We see that the 2-cycle is broken and the point $R^2_\beta(\varrho_+(\beta))$ has been slightly moved to the left. On the right, graph or $R_\beta(y)$ for $\beta = 1.30$. In this case, the image of $R^2_\beta(\varrho_+(\beta))$ is near the maximum of the function $R_\beta(y)$.

$R^n_{\hat\beta_n}(\varrho_+(\hat\beta_n)) = \varrho_-(\hat\beta_n)$. Then

$$R^{n+1}_{\hat\beta_n}(\varrho_+(\hat\beta_n)) = R_{\hat\beta_n}(\varrho_-(\hat\beta_n)) > \hat\beta_n > \varrho_+(\hat\beta_n)$$

and $g_{n+1}(\hat\beta_n) > 0$. Once again, this process can be seen in Figures 5 and 6. The continuity of $g_{n+1}(\beta)$ on $[0, \sqrt{3})$ and the fact

$$\lim_{\beta \to \sqrt{3}^-} g_{n+1}(\beta) = -\infty,$$

guarantee the existence of β_{n+1}. As in the previous cases, we always choose β_{n+1} as the biggest of the solutions of $g_{n+1}(\beta) = 0$.

The last part of the theorem follows from the fact that the image by $R_\beta(y)$ of the critical point $\varrho_+(\beta)$ is strictly decreasing for $\beta > \beta^*$. In addition, for values of y negative and large in magnitude, $R_\beta(y)$ can be approximated by the asymptote $5y/9 + 4\beta/27$, so the orbit of the free critical point $\varrho_+(\beta_{n+1})$ needs more and more iterates to return back near itself. Therefore, the larger is the period of the superattracting n-cycle, the more negative must be the image of $R_\beta(\varrho_+(\beta))$ and the closer β must be to $\sqrt{3}$. □

Remark 2. If we define $\lambda_n = \beta_n i$, with β_n given in Theorem 4, then Chebyshev's method applied to $(z^2 - 1)(z - \lambda_n)$ has a superattracting n-cycle. This cycle is obtained by following the orbit of the free critical value $\rho_+(\lambda_n)$. In addition, as a direct consequence of Lemma 3, the orbit of the other free critical point, $\rho_-(\lambda_n)$ converges in these cases to the root $\lambda_n = \beta_n i$.

The values in Table 2 give rise to a "channel" of superattracting n-cycles in the parameter plane showed in Figure 1, moving around the imaginary axis towards the point $\sqrt{3}i \approx 1.73205i$. In Figure 7 we show this channel, together a magnification around $\beta_2 i \approx 1.28657i$.

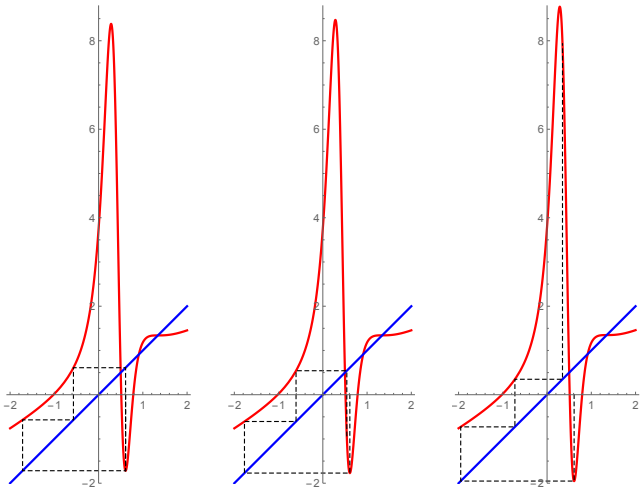

Figure 6: On the left, graph or $R_\beta(y)$ for $\beta = \beta_3 \approx 1.34015$ together with the web diagram proving the existence of a superattracting 3-cycle containing the free critical point $\varrho_+(\beta_3)$. In the middle, graph or $R_\beta(y)$ for $\beta = 1.342$. We see that the 3-cycle is broken and the point $R^3_\beta(\varrho_+(\beta))$ has been slightly moved to the left. On the right, graph or $R_\beta(y)$ for $\beta = 1.348$. In this case, the image of $R^3_\beta(\varrho_+(\beta))$ is near the maximum of the function $R_\beta(y)$.

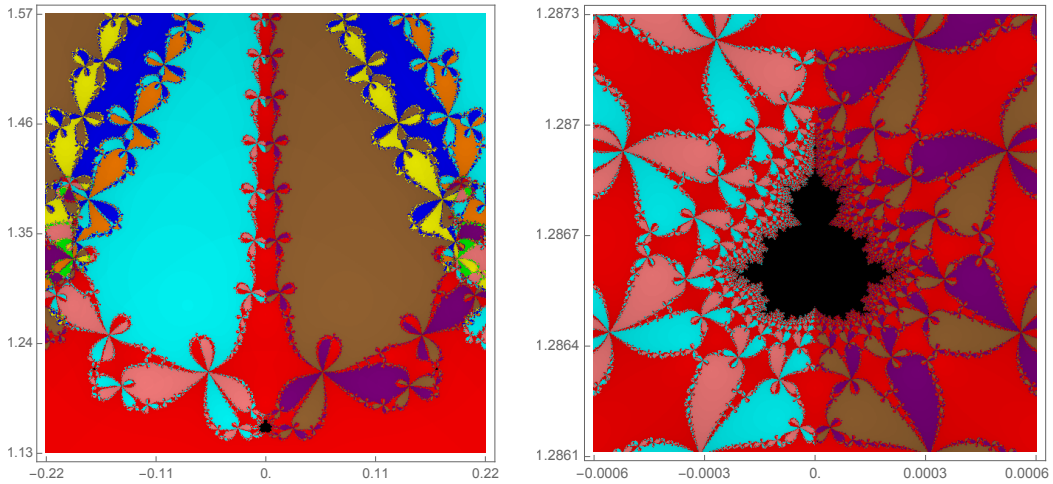

Figure 7: On the left, a channel of black holes (around the imaginary axis) created by the presence of superattracting n-cycles, in the rectangle $[-0.22, 0.22] \times [1.13, 1.57]$ of the parameter plane (note that the black hole on the bottom is just the one that appears on Figure 2-left, coming from the superattracting extraneous fixed point $\frac{2\sqrt{3}}{3}\, i$). On the right, a detail in the rectangle $[-0.0006, 0.0006] \times [1.2861, 1.2873]$ showing a black hole coming from a superattracting 2-cycle.

Remark 3. In this section, we have only studied in detail the above channel of superattracting n-cycles associated to $\beta_n i$, $n \geq 2$. This case is easier, because the $\beta_n i$ lie on the imaginary axis and thus it can be analyzed as an 1-dimensional problem. However, other channels of superattracting n-cycles exist in the parameter plane. For instance, three channels of superattracting n-cycles arise from the central point $\sqrt{3}i$ of Figure 1-right, between adjacent pairs of "petals" in the central "flower". The channel that goes downwards is associated to the points $\beta_n i$, $n \geq 2$, and we have seen it in Figure 7. There is another channel of superattracting n-cycles associated to λ_n, $n \geq 2$, that goes leftwards (and, of course, there is a third channel that goes rightwards).

Note that there is an inherent symmetry in the structure of the parameter plane showed in Figure 1 that can be explained by means of the two affine conjugacies introduced in Section 2.1. We can see the channel that goes leftwards in Figure 8. It is formed by the images of $\beta_n i$ under the map defined in (8), that is $\lambda_n = (\beta_n i - 3)/(1 + \beta_n i)$. The first values of the corresponding λ_n are $\lambda_2 \approx -0.506445 + 1.93814i$, $\lambda_3 \approx -0.430614 + 1.91724i$, $\lambda_4 \approx -0.364954 + 1.89650i$, $\lambda_5 \approx -0.304138 + 1.87504i$ and $\lambda_6 \approx -0.249473 + 1.85384i$.

In a similar way the channel that goes rightwards in Figure 8 is formed by the images of $\beta_n i$ under the map defined in (9), that is $\lambda_n = (\beta_n i + 3)/(1 - \beta_n i)$. In this way we obtain a list of values of λ that are the complex conjugated of the listed above.

As a final conclusion, we see that each channel of superattracting n-cycles can be found by applying a linear fractional transformation (e.g., equations (8) or (9)) to the main channel running along the imaginary axis.

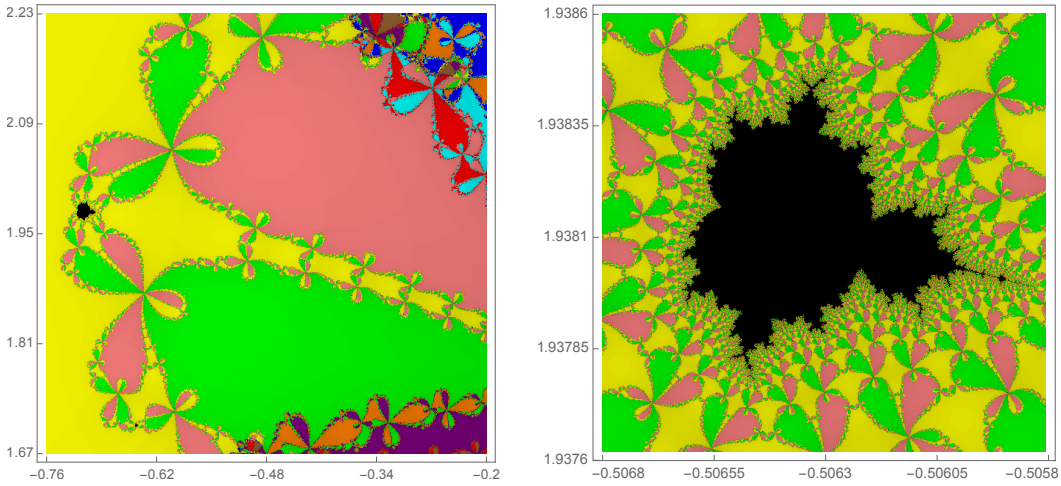

Figure 8: On the left, a channel of black holes created by the presence of superattracting n-cycles, in the rectangle $[-0.76, -0.20] \times [1.67, 2.23]$ of the parameter plane (note that the black hole on the left is just the one that appears on Figure 2-right, coming from the superattracting extraneous fixed point $\frac{-5+8\sqrt{3}i}{7}$). On the right, a detail in the rectangle $[-0.5068, -0.5058] \times [1.9376, 1.9386]$ showing a black hole coming from a superattracting 2-cycle.

3 Dynamical planes

We end this paper showing the dynamical planes related to Chebyshev's method applied to a couple of polynomials $p_\lambda(z)$ that belong to the classes mentioned in the previous section. In these dynamical planes we show, for each polynomial, the Julia and Fatou sets associated with the rational map $C_{p_\lambda}(z)$ defined in (1). In particular, the basins of attraction of the roots of $p_\lambda(z)$ are represented, as a part of the Fatou set. These basins are the sets of initial points $z_0 \in \mathbb{C}$ such that the orbit of z_0 under iteration by $C_{p_\lambda}(z)$ converges to a root of $p_\lambda(z)$. We see that in the considered polynomials, other kind of sets appear in the Fatou set in addition to the basins of the roots.

Firstly, we have chosen $\lambda_1 = (-5 + 8\sqrt{3}i)/7$. In this case, Chebyshev's method applied to $p_{\lambda_1}(z) = (z^2 - 1)(z - \lambda_1)$ has a superattracting extraneous fixed point at $\rho_-(\lambda_1) = \left(5\lambda_1 - \sqrt{-5(\lambda_1^2 + 3)}\right)/15 \approx -0.428571 + 0.494872i$ (we have already shown the parameter plane around this point in Figure 2-right). There are other extraneous fixed points, but they are repelling. In the left side of Figure 9 we show the dynamical plane of Chebyshev's map $C_{p_{\lambda_1}}(z)$. Together with the basins of attraction of the three roots 1, -1 and λ_1 (coloured in yellow, magenta and cyan respectively, and with black assigned to the points such that the iterative method starting in them does not converge), a white region appears. Actually, this white region is contained in the basin of attraction of the superattracting extraneous fixed point $\rho_-(\lambda_1)$. In fact, it is its immediate basin of attraction. Notice that the boundary of this basin does not present a fractal structure, as in the case of the boundaries of the basins of the roots. Other components of the basin of $\rho_-(\lambda_1)$ can be also seen in the left side of Figure 9 (tiny white zones). In the right side of this same figure we show a magnification of the dynamical plane around one of these components of the same basin of attraction.

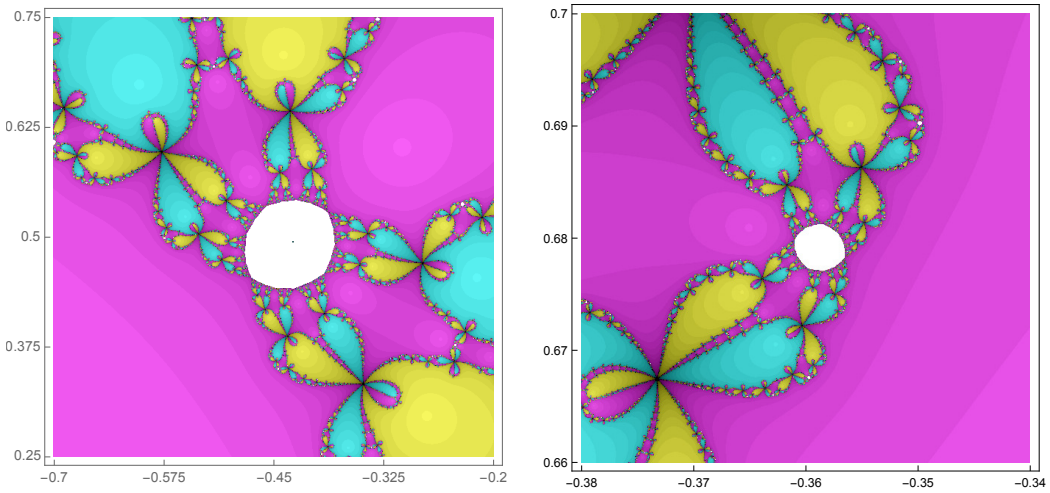

Figure 9: On the left, a detail of the dynamical plane of Chebyshev's map $C_{p_{\lambda_1}}(z)$, where $\lambda_1 = \left(-5 + 8\sqrt{3}i\right)/7$. It is plotted in the rectangle $[-0.7, -0.2] \times [0.25, 0.75]$ of the complex plane. A part of the basin of attraction of the superattracting extraneous fixed point $\rho_-(\lambda_1) = \left(-3 + 2\sqrt{3}i\right)/7 \approx -0.428571 + 0.494872i$ is coloured in white. On the right, a zoom around another component of the same basin of attraction, namely the rectangle $[-0.38, -0.34] \times [0.66, 0.70]$.

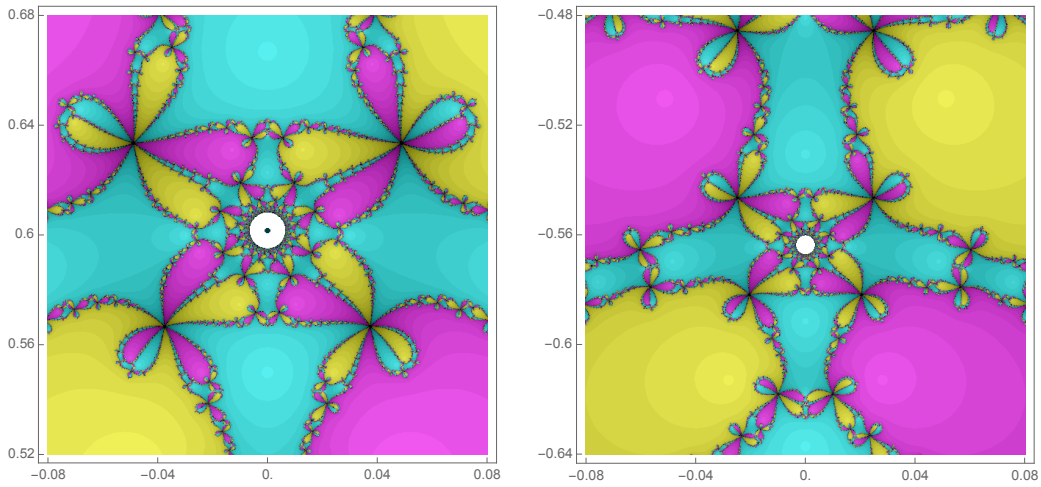

Figure 10: On the left, a detail of the dynamical plane of Chebyshev's map $C_{p_{\lambda_2}}(z)$, where $\lambda_2 = \beta_2 i$ and $\beta_2 \approx 1.28657$ (see Table 2). It is plotted in the rectangle $[-0.08, 0.08] \times [0.52, 0.68]$ of the complex plane. A part of the basin of attraction of the superattracting 2-cycle around $\rho_+(\lambda_2) \approx 0.601724i$ is coloured in white. On the right, the dynamical plane on the rectangle $[-0.08, 0.08] \times [-0.64, -0.48]$, that contains another component of the superattracting 2-cycle.

Secondly, we consider Chebyshev's method applied to $p_{\lambda_2}(z) = (z^2 - 1)(z - \lambda_2)$ where $\lambda_2 = \beta_2 i$ and $\beta_2 \approx 1.28657$ (see Table 2). In this case, Chebyshev's map $C_{p_{\lambda_2}}(z)$ has a superattracting 2-cycle, as we have already shown in the parameter plane around this point in Figure 7-right. In the left side of Figure 10 we have plotted the dynamical plane of Chebyshev's map $C_{p_{\lambda_2}}(z)$. We see the basins of attraction of the three roots 1, -1 and λ_2 (coloured again in yellow, magenta and cyan respectively, and black for non-convergent points), and a white region that corresponds in this case with a part of the basin of attraction of the 2-cycle generated by the orbit of the free critical point $\rho_+(\lambda_2) = \left(5\lambda_2 + \sqrt{-5(\lambda_2^2 + 3)}\right)/15 \approx 0.601724i$. As in the previous situation, we note that the boundary of this basin has the shape of a simple closed curve, not as in the case of the intricate boundaries of the basins of the roots. Note that in the study of dynamical planes with 2-cycles, each basin has a "twin component" corresponding to the other element of the 2-cycle, in this case, around $-0.563617i$. This "twin component" is shown in the right side of Figure 10.

We have seen that Chebyshev's method applied to $p_{\lambda_1}(z)$ has a superattracting fixed point, and that Chebyshev's method applied to $p_{\lambda_2}(z)$ has a superattracting 2-cycle. It is interesting to note that, for values of λ close enough to λ_1 or λ_2, we obtain attracting but not superattracting fixed points or 2-cycles.

Let us first analyze the case of λ close enough to $\lambda_1 = (-5 + 8\sqrt{3}i)/7 \approx -0.714286 + 1.97949i$, for instance $\lambda = -0.71 + 1.98i$. Now, Chebyshev's method applied to $p_\lambda(z) = (z^2 - 1)(z - \lambda)$ has an attracting (but not superattracting) extraneous fixed point at $-0.42019 + 0.504969i$ with

$$|C'_{p_\lambda}(-0.42019 + 0.504969i)| = 0.484302.$$

As in the previous case, C_{p_λ} has other extraneous fixed points, but all of them are repelling. The dynamical plane of this case appears in the left side of Figure 11 (observe that the picture is very

similar to the one that appears in the left side of Figure 9, although we have now used a smaller rectangle).

For values of λ close enough to $\lambda_2 = \beta_2 i \approx 1.28657i$, for instance $\lambda = 1.2866i$, Chebyshev's method applied to $p_\lambda(z) = (z^2-1)(z-\lambda)$ has an attracting (but not superattracting) 2-cycle: $\{-0.564038i, 0.60089i\}$ with multiplier $C'_{p_\lambda}(-0.564038i)C'_{p_\lambda}(0.60089i) = -0.259423$. A part of the dynamical plane of this situation is shown in the right side of Figure 11 (observe that the picture is very similar to the one that appears in the left side of Figure 10, but with a smaller rectangle).

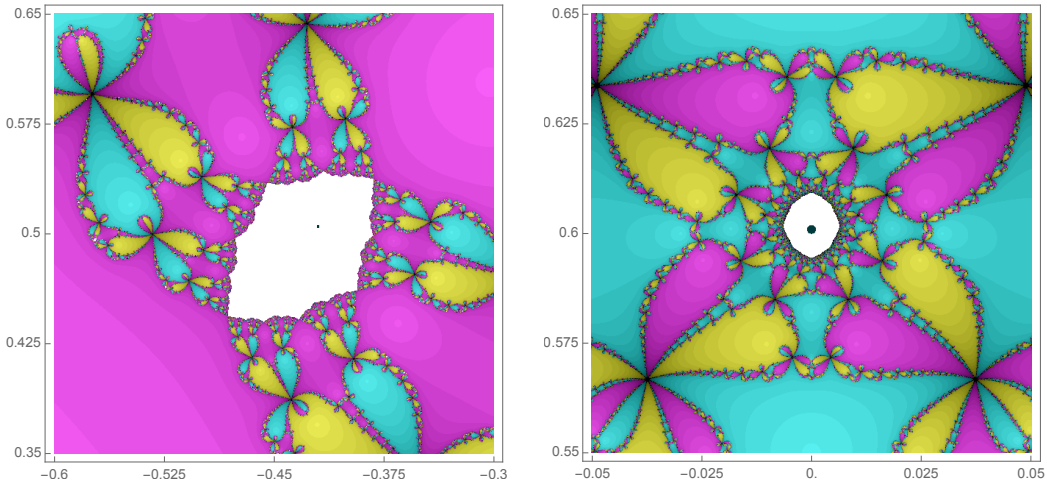

Figure 11: On the left, the dynamical plane of Chebyshev's map $C_{p_\lambda}(z)$ for $\lambda = -0.71 + 1.08i$. It is plotted in the rectangle $[-0.6, -0.3] \times [0.35, 0.65]$ of the complex plane. A part of the basin of attraction of the attracting extraneous fixed point $-0.42019 + 0.504969i$ is coloured in white. On the right, the dynamical plane of Chebyshev's map $C_{p_\lambda}(z)$ for $\lambda = 1.2866i$. It is plotted in the rectangle $[-0.05, 0.05] \times [0.55, 0.65]$ of the complex plane. A part of the basin of attraction of the attracting 2-cycle $\{-0.564038i, 0.60089i\}$ is coloured in white.

Acknowledgements

This research was partially supported by Ministerio de Ciencia, Innovación y Universidades under grants PGC2018-095896-B-C21 and PGC2018-096504-B-C32. The authors want to acknowledge the helpful, constructive and detailed revision of the manuscript by the referees, that has allowed us to improve the final version of the paper.

References

[1] S. Amat, S. Busquier and S. Plaza, Review of some iterative root-finding methods from a dynamical point of view, *SCIENTIA, Series A: Math. Sciences* **10** (2004), 3–35.

[2] I. K. Argyros and S. Hilout, *Computational Methods in Nonlinear Analysis: Efficient Algorithms, Fixed Point Theory and Applications*, World Scientific, Singapore, 2013.

[3] A. F. Beardon, *Iteration of rational functions*, Springer-Verlag, New York, 1991.

[4] P. Blanchard, D. Cuzzocreo, R. L. Devaney and E. Fitzgibbon, Accessible Mandelbrot sets in the family $z^n + \lambda/z^n$, *Qual. Theory Dyn. Syst.* **15** (2016), no. 1, 49–66.

[5] A. Cordero, J. R. Torregrosa and P. Vindel, Bulbs of period two in the family of Chebyshev-Halley iterative methods on quadratic polynomials, *Abstr. Appl. Anal.* **2013** (2013), Article ID 536910, 1–10.

[6] A. Cordero, J. R. Torregrosa and P. Vindel, Dynamics of a family of Chebyshev-Halley type methods, *Appl. Math. Comput.* **219** (2013), no. 16, 8568–8583.

[7] J. H. Curry, L. Garnett and D. Sullivan, On the iteration of a rational function: computer experiments with Newton's method, *Comm. Math. Phys.* **91** (1983), no. 2, 267–277.

[8] M. A. Diloné, M. García-Olivo and J. M. Gutiérrez, A note on the semilocal convergence of Chebyshev's method, *Bull. Austral. Math. Soc.* **88** (2013), no. 1, 98–105.

[9] M. García-Olivo, J. M. Gutiérrez and Á. A. Magreñán, A complex dynamical approach of Chebyshev's method, *SeMA Journal* **71** (2015), no. 1, 57–68.

[10] J. M. Gutiérrez, The Cayley problem and the Chebyshev method (Spanish), *Gac. R. Soc. Mat. Esp.* **19** (2016), no. 3, 542.

[11] K. Kneisl, Julia sets for the super-Newton method, Cauchy's method and Halley's method, *Chaos* **11** (2001), no. 2, 359–370.

[12] M. Yu. Lyubich, The dynamics of rational transforms: the topological picture, *Russian Math. Surveys* **41** (1986), no. 4, 43–117.

[13] C. McMullen, Families of rational maps and iterative root-finding algorithms, *Ann. of Math. (2)* **125** (1987), no. 3, 467–493.

[14] C. McMullen, The Mandelbrot set is universal, *The Mandelbrot set, theme and variations*, London Math. Soc. Lecture Note Ser., 274, pp. 1–17, Cambridge Univ. Press, Cambridge, 2000.

[15] J. Milnor, *Dynamics in one complex variable*, Third edition, Annals of Mathematics Studies, 160, Princeton University Press, Princeton, NJ, 2006.

[16] G. E. Roberts and J. Horgan-Kobelski, Newton's versus Halley's methods: a dynamical systems approach, *Internat. J. Bifur. Chaos Appl. Sci. Engrg.* **14** (2004), no. 10, 3459–3475.

[17] S. Smale, On the efficiency of algorithms of analysis, *Bull. Amer. Math. Soc. (N.S.)* **13** (1985), no. 2, 87–121.

[18] J. L. Varona, Graphic and numerical comparison between iterative methods, *Math. Intelligencer* **24** (2002), no. 1, 37–46.

[19] E. R. Vrscay, Julia sets and Mandelbrot-like sets associated with higher order Schröder rational iteration functions: a computer assisted study, *Math. Comp.* **46** (1986), no. 173, 151–169.

[20] E. R. Vrscay and W. J. Gilbert, Extraneous fixed points, basin boundaries and chaotic dynamics for Schröder and König rational iteration functions, *Numer. Math.* **52** (1988), no. 1, 1–16.

[21] J. Walsh, The dynamics of Newton's method for cubic polynomials, *College Math. J.* **26** (1995), no. 1, 22–28.